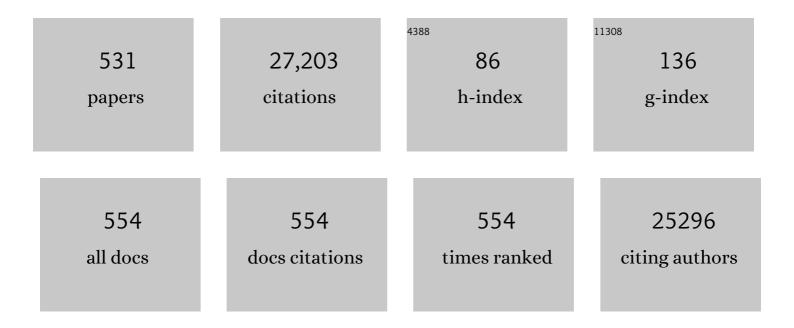
List of Publications by Year in descending order

Source: https://exaly.com/author-pdf/886093/publications.pdf Version: 2024-02-01



MISCHA RONN

#	Article	IF	CITATIONS
1	Untying the Bundles of Solution‣ynthesized Graphene Nanoribbons for Highly Capacitive Micro‣upercapacitors. Advanced Functional Materials, 2022, 32, 2109543.	14.9	13
2	Tuning interfacial charge transfer in atomically precise nanographene–graphene heterostructures by engineering van der Waals interactions. Journal of Chemical Physics, 2022, 156, 074702.	3.0	5
3	Toward Understanding Bacterial Ice Nucleation. Journal of Physical Chemistry B, 2022, 126, 1861-1867.	2.6	24
4	Ice Recrystallization Inhibition Is Insufficient to Explain Cryopreservation Abilities of Antifreeze Proteins. Biomacromolecules, 2022, 23, 1214-1220.	5.4	17
5	Electrochemical Deposition of a Singleâ€Crystalline Nanorod Polycyclic Aromatic Hydrocarbon Film with Efficient Charge and Exciton Transport. Angewandte Chemie, 2022, 134, .	2.0	3
6	Accurate molecular orientation at interfaces determined by multimode polarization-dependent heterodyne-detected sum-frequency generation spectroscopy via multidimensional orientational distribution function. Journal of Chemical Physics, 2022, 156, 094703.	3.0	12
7	Redoxâ€Active Metaphosphateâ€Like Terminals Enable Highâ€Capacity MXene Anodes for Ultrafast Naâ€Ion Storage. Advanced Materials, 2022, 34, e2108682.	21.0	52
8	Electrochemical Deposition of a Singleâ€Crystalline Nanorod Polycyclic Aromatic Hydrocarbon Film with Efficient Charge and Exciton Transport. Angewandte Chemie - International Edition, 2022, 61, .	13.8	14
9	High-Performance Humidity Sensing in π-Conjugated Molecular Assemblies through the Engineering of Electron/Proton Transport and Device Interfaces. Journal of the American Chemical Society, 2022, 144, 2546-2555.	13.7	17
10	Passively Stabilized Phase-Resolved Collinear SFG Spectroscopy Using a Displaced Sagnac Interferometer. Journal of Physical Chemistry A, 2022, 126, 951-956.	2.5	3
11	The role of structural order in heterogeneous ice nucleation. Chemical Science, 2022, 13, 5014-5026.	7.4	10
12	Small Size, Big Impact: Recent Progress in Bottomâ€Up Synthesized Nanographenes for Optoelectronic and Energy Applications. Advanced Science, 2022, 9, e2106055.	11.2	54
13	Band transport by large Fröhlich polarons in MXenes. Nature Physics, 2022, 18, 544-550.	16.7	40
14	Solution Synthesis and Characterization of a Long and Curved Graphene Nanoribbon with Hybrid Cove–Armchair–Gulf Edge Structures. Advanced Science, 2022, 9, e2200708.	11.2	12
15	Cove-Edged Graphene Nanoribbons with Incorporation of Periodic Zigzag-Edge Segments. Journal of the American Chemical Society, 2022, 144, 228-235.	13.7	28
16	A Nanographeneâ€Based Twoâ€Dimensional Covalent Organic Framework as a Stable and Efficient Photocatalyst. Angewandte Chemie - International Edition, 2022, 61, .	13.8	38
17	A Nanographeneâ€Based Twoâ€Đimensional Covalent Organic Framework as a Stable and Efficient Photocatalyst. Angewandte Chemie, 2022, 134, .	2.0	2
18	Outstanding Charge Mobility by Band Transport in Two-Dimensional Semiconducting Covalent Organic Frameworks. Journal of the American Chemical Society, 2022, 144, 7489-7496.	13.7	43

#	Article	IF	CITATIONS
19	Solutionâ€Processed Waferâ€Scale Ag ₂ S Thin Films: Synthesis and Excellent Charge Transport Properties. Advanced Functional Materials, 2022, 32, .	14.9	3
20	Wettability of graphene, water contact angle, and interfacial water structure. CheM, 2022, 8, 1187-1200.	11.7	18
21	Polarization-Dependent Sum-Frequency Generation Spectroscopy for Ã…ngstrom-Scale Depth Profiling of Molecules at Interfaces. Physical Review Letters, 2022, 128, .	7.8	8
22	Phospholipid acyl tail affects lipid headgroup orientation and membrane hydration. Journal of Chemical Physics, 2022, 156, .	3.0	7
23	Probing Carrier Dynamics in <i>sp</i> ³ -Functionalized Single-Walled Carbon Nanotubes with Time-Resolved Terahertz Spectroscopy. ACS Nano, 2022, 16, 9401-9409.	14.6	12
24	Polarization-Dependent Heterodyne-Detected Sum-Frequency Generation Spectroscopy as a Tool to Explore Surface Molecular Orientation and Ångström-Scale Depth Profiling. Journal of Physical Chemistry B, 2022, 126, 6113-6124.	2.6	11
25	Acidic pH Promotes Refolding and Macroscopic Assembly of Amyloid β (16–22) Peptides at the Air–Water Interface. Journal of Physical Chemistry Letters, 2022, 13, 6674-6679.	4.6	3
26	Probing the Mineral–Water Interface with Nonlinear Optical Spectroscopy. Angewandte Chemie - International Edition, 2021, 60, 10482-10501.	13.8	56
27	Probing fibrin's molecular response to shear and tensile deformation with coherent Raman microscopy. Acta Biomaterialia, 2021, 121, 383-392.	8.3	16
28	Grating-Graphene Metamaterial as a Platform for Terahertz Nonlinear Photonics. ACS Nano, 2021, 15, 1145-1154.	14.6	69
29	Interfacial Water Ordering Is Insufficient to Explain Ice-Nucleating Protein Activity. Journal of Physical Chemistry Letters, 2021, 12, 218-223.	4.6	15
30	Untersuchung der Mineralâ€Wasserâ€Grenzschicht mit nichtâ€linearer optischer Spektroskopie. Angewandte Chemie, 2021, 133, 10574-10595.	2.0	3
31	WATER AT INTERFACES: WHERE THEORY NEEDS TO MEET EXPERIMENT. , 2021, , .		0
32	Role of Water in CaCO ₃ Biomineralization. Journal of the American Chemical Society, 2021, 143, 1758-1762.	13.7	28
33	Long-lived charge separation following pump-wavelength–dependent ultrafast charge transfer in graphene/WS ₂ heterostructures. Science Advances, 2021, 7, .	10.3	60
34	Specific Ion–Protein Interactions Influence Bacterial Ice Nucleation. Chemistry - A European Journal, 2021, 27, 7402-7407.	3.3	20
35	lce Nucleation Activity of Perfluorinated Organic Acids. Journal of Physical Chemistry Letters, 2021, 12, 3431-3435.	4.6	7
36	Synthesis of Nonplanar Graphene Nanoribbon with Fjord Edges. Journal of the American Chemical Society, 2021, 143, 5654-5658.	13.7	52

#	Article	IF	CITATIONS
37	Electrical tunability of terahertz nonlinearity in graphene. Science Advances, 2021, 7, .	10.3	52
38	Distinguishing different excitation pathways in two-dimensional terahertz-infrared-visible spectroscopy. Journal of Chemical Physics, 2021, 154, 174201.	3.0	8
39	Antisurfactant (Autophobic) Behavior of Superspreader Surfactant Solutions. Langmuir, 2021, 37, 6243-6247.	3.5	7
40	Disentangling Sum-Frequency Generation Spectra of the Water Bending Mode at Charged Aqueous Interfaces. Journal of Physical Chemistry B, 2021, 125, 7060-7067.	2.6	18
41	Hot-Carrier Cooling in High-Quality Graphene Is Intrinsically Limited by Optical Phonons. ACS Nano, 2021, 15, 11285-11295.	14.6	43
42	Water at charged interfaces. Nature Reviews Chemistry, 2021, 5, 466-485.	30.2	186
43	Intrinsisch ungeordnete Osteopontinâ€Fragmente ordnen sich wĤrend der interfazialen Calciumoxalatâ€Mineralisierung. Angewandte Chemie, 2021, 133, 18725-18729.	2.0	0
44	Intrinsically Disordered Osteopontin Fragment Orders During Interfacial Calcium Oxalate Mineralization. Angewandte Chemie - International Edition, 2021, 60, 18577-18581.	13.8	6
45	A Highly Luminescent Nitrogen-Doped Nanographene as an Acid- and Metal-Sensitive Fluorophore for Optical Imaging. Journal of the American Chemical Society, 2021, 143, 10403-10412.	13.7	37
46	Liquid flow reversibly creates a macroscopic surface charge gradient. Nature Communications, 2021, 12, 4102.	12.8	19
47	<i>In Situ</i> Label-Free Study of Protein Adsorption on Nanoparticles. Journal of Physical Chemistry B, 2021, 125, 9019-9026.	2.6	12
48	Water Orientation at the Calcite-Water Interface. Journal of Physical Chemistry Letters, 2021, 12, 7605-7611.	4.6	16
49	Real-time study of on-water chemistry: Surfactant monolayer-assisted growth of a crystalline quasi-2D polymer. CheM, 2021, 7, 2758-2770.	11.7	23
50	Bandâ€Like Charge Transport in Phytic Acidâ€Doped Polyaniline Thin Films. Advanced Functional Materials, 2021, 31, 2105184.	14.9	22
51	Low-field onset of Wannier-Stark localization in a polycrystalline hybrid organic inorganic perovskite. Nature Communications, 2021, 12, 5719.	12.8	6
52	Molecularly Engineered Black Phosphorus Heterostructures with Improved Ambient Stability and Enhanced Charge Carrier Mobility. Advanced Materials, 2021, 33, e2105694.	21.0	16
53	Interfacial Water Structure of Binary Liquid Mixtures Reflects Nonideal Behavior. Journal of Physical Chemistry B, 2021, 125, 10639-10646.	2.6	8
54	Exceptional electron conduction in two-dimensional covalent organic frameworks. CheM, 2021, 7, 3309-3324.	11.7	41

#	Article	IF	CITATIONS
55	Assembly of iron oxide nanosheets at the air–water interface by leucine–histidine peptides. RSC Advances, 2021, 11, 27965-27968.	3.6	3
56	Between a hydrogen and a covalent bond. Science, 2021, 371, 123-124.	12.6	28
57	Highly Mobile Large Polarons in Black Phase CsPbI ₃ . ACS Energy Letters, 2021, 6, 568-573.	17.4	40
58	Protein Nanopore Membranes Prepared by a Simple Langmuir–Schaefer Approach. Small, 2021, 17, e2102975.	10.0	3
59	Interfacial Vibrational Spectroscopy of the Water Bending Mode on Ice <i>I_h</i> . Journal of Physical Chemistry C, 2021, 125, 22937-22942.	3.1	4
60	Solution-Processed Graphene–Nanographene van der Waals Heterostructures for Photodetectors with Efficient and Ultralong Charge Separation. Journal of the American Chemical Society, 2021, 143, 17109-17116.	13.7	19
61	Membranes Are Decisive for Maximum Freezing Efficiency of Bacterial Ice Nucleators. Journal of Physical Chemistry Letters, 2021, 12, 10783-10787.	4.6	10
62	Membrane Structure of Aquaporin Observed with Combined Experimental and Theoretical Sum Frequency Generation Spectroscopy. Langmuir, 2021, 37, 13452-13459.	3.5	4
63	Highly mobile hot holes in Cs ₂ AgBiBr ₆ double perovskite. Science Advances, 2021, 7, eabj9066.	10.3	21
64	Nanographene: ultrastabile, schaltbare und helle Sonden für die hochauflösende Mikroskopie. Angewandte Chemie, 2020, 132, 504-510.	2.0	4
65	Terahertz Nonlinear Optics of Graphene: From Saturable Absorption to Highâ€Harmonics Generation. Advanced Optical Materials, 2020, 8, 1900771.	7.3	97
66	Nanographenes: Ultrastable, Switchable, and Bright Probes for Superâ€Resolution Microscopy. Angewandte Chemie - International Edition, 2020, 59, 496-502.	13.8	35
67	Room-temperature solution-phase epitaxial nucleation of PbS quantum dots on rutile TiO ₂ (100). Nanoscale Advances, 2020, 2, 377-383.	4.6	2
68	Interfacial Approach toward Benzeneâ€Bridged Polypyrrole Film–Based Microâ€6upercapacitors with Ultrahigh Volumetric Power Density. Advanced Functional Materials, 2020, 30, 1908243.	14.9	60
69	Nature of Excess Hydrated Proton at the Water–Air Interface. Journal of the American Chemical Society, 2020, 142, 945-952.	13.7	41
70	Use of Ion Exchange To Regulate the Heterogeneous Ice Nucleation Efficiency of Mica. Journal of the American Chemical Society, 2020, 142, 17956-17965.	13.7	26
71	A Curved Graphene Nanoribbon with Multi-Edge Structure and High Intrinsic Charge Carrier Mobility. Journal of the American Chemical Society, 2020, 142, 18293-18298.	13.7	50
72	Bottom-Up, On-Surface-Synthesized Armchair Graphene Nanoribbons for Ultra-High-Power Micro-Supercapacitors. Journal of the American Chemical Society, 2020, 142, 17881-17886.	13.7	51

#	Article	IF	CITATIONS
73	Size-dependent electron transfer from atomically defined nanographenes to metal oxide nanoparticles. Nanoscale, 2020, 12, 16046-16052.	5.6	6
74	Photoconductivity Multiplication in Semiconducting Few-Layer MoTe ₂ . Nano Letters, 2020, 20, 5807-5813.	9.1	45
75	Tuning the Structural and Optoelectronic Properties of Cs ₂ AgBiBr ₆ Doubleâ€Perovskite Single Crystals through Alkaliâ€Metal Substitution. Advanced Materials, 2020, 32, e2001878.	21.0	72
76	The Bending Mode of Water: A Powerful Probe for Hydrogen Bond Structure of Aqueous Systems. Journal of Physical Chemistry Letters, 2020, 11, 8459-8469.	4.6	175
77	Ultrafast terahertz magnetometry. Nature Communications, 2020, 11, 4247.	12.8	61
78	Geopolymer-Encapsulated Cesium Lead Bromide Perovskite Nanocrystals for Potential Display Applications. ACS Applied Nano Materials, 2020, 3, 11695-11700.	5.0	6
79	Tension Causes Unfolding of Intracellular Vimentin Intermediate Filaments. Advanced Biology, 2020, 4, e2000111.	3.0	7
80	High-Mobility Semiconducting Two-Dimensional Conjugated Covalent Organic Frameworks with <i>p</i> -Type Doping. Journal of the American Chemical Society, 2020, 142, 21622-21627.	13.7	113
81	Vibrational couplings and energy transfer pathways of water's bending mode. Nature Communications, 2020, 11, 5977.	12.8	50
82	Orientation independent vibrational dynamics of lipid-bound interfacial water. Physical Chemistry Chemical Physics, 2020, 22, 10142-10148.	2.8	7
83	Inhibition of Bacterial Ice Nucleators Is Not an Intrinsic Property of Antifreeze Proteins. Journal of Physical Chemistry B, 2020, 124, 4889-4895.	2.6	17
84	Vibrational mode frequency correction of liquid water in density functional theory molecular dynamics simulations with van der Waals correction. Physical Chemistry Chemical Physics, 2020, 22, 12785-12793.	2.8	9
85	Charge carrier scattering and ultrafast Auger dynamics in two-dimensional superatomic semiconductors. Applied Physics Letters, 2020, 116, 201109.	3.3	1
86	Interfacial Vibrational Dynamics of Ice I _h and Liquid Water. Journal of the American Chemical Society, 2020, 142, 12005-12009.	13.7	11
87	Bridging chains mediate nonlinear mechanics of polymer nanocomposites under cyclic deformation. Polymer, 2020, 200, 122529.	3.8	3
88	Dynamic Surface Tension of Surfactants in the Presence of High Salt Concentrations. Langmuir, 2020, 36, 7956-7964.	3.5	81
89	Thickness-dependent electron momentum relaxation times in iron films. Applied Physics Letters, 2020, 116, .	3.3	5
90	Kinetic Control over Self-Assembly of Semiconductor Nanoplatelets, Nano Letters, 2020, 20, 4102-4110	91	57

#	Article	IF	CITATIONS
91	OberflÜhenladungen an der CaF 2 â€Wasserâ€GrenzflÃæhe erlauben eine sehr schnelle intermolekulare Übertragung von Schwingungsenergie. Angewandte Chemie, 2020, 132, 13217-13222.	2.0	2
92	Electrostatic Interactions Control the Functionality of Bacterial Ice Nucleators. Journal of the American Chemical Society, 2020, 142, 6842-6846.	13.7	33
93	Macroscopic conductivity of aqueous electrolyte solutions scales with ultrafast microscopic ion motions. Nature Communications, 2020, 11, 1611.	12.8	31
94	Molecular Structure and Modeling of Water–Air and Ice–Air Interfaces Monitored by Sum-Frequency Generation. Chemical Reviews, 2020, 120, 3633-3667.	47.7	97
95	Rücktitelbild: Nanographene: ultrastabile, schaltbare und helle Sonden für die hochauflösende Mikroskopie (Angew. Chem. 1/2020). Angewandte Chemie, 2020, 132, 516-516.	2.0	0
96	Charge transport mechanism in networks of armchair graphene nanoribbons. Scientific Reports, 2020, 10, 1988.	3.3	41
97	Hysteresis in graphene nanoribbon field-effect devices. Physical Chemistry Chemical Physics, 2020, 22, 5667-5672.	2.8	9
98	Structure and Dynamics of Interfacial Peptides and Proteins from Vibrational Sum-Frequency Generation Spectroscopy. Chemical Reviews, 2020, 120, 3420-3465.	47.7	114
99	Highly Crystalline and Semiconducting Imineâ€Based Twoâ€Dimensional Polymers Enabled by Interfacial Synthesis. Angewandte Chemie, 2020, 132, 6084-6092.	2.0	18
100	Compositionâ€Đependent Passivation Efficiency at the CdS/CuIn 1- x Ga x Se 2 Interface. Advanced Materials, 2020, 32, 1907763.	21.0	7
101	Highly Crystalline and Semiconducting Imineâ€Based Twoâ€Dimensional Polymers Enabled by Interfacial Synthesis. Angewandte Chemie - International Edition, 2020, 59, 6028-6036.	13.8	98
102	Surface Charges at the CaF ₂ /Water Interface Allow Very Fast Intermolecular Vibrationalâ€Energy Transfer. Angewandte Chemie - International Edition, 2020, 59, 13116-13121.	13.8	14
103	Decoding the molecular water structure at complex interfaces through surface-specific spectroscopy of the water bending mode. Physical Chemistry Chemical Physics, 2020, 22, 10934-10940.	2.8	11
104	Frequency-domain study of nonthermal gigahertz phonons reveals Fano coupling to charge carriers. Science Advances, 2020, 6, .	10.3	11
105	Kinetic Ionic Permeation and Interfacial Doping of Supported Graphene Measured with Terahertz Photoconductivity Measurements. , 2020, , .		0
106	Ultrafast carrier dynamics in graphene and graphene nanostructures. Terahertz Science & Technology, 2020, 13, 135-148.	0.5	1
107	Water-Dispersed High-Quality Graphene: A Green Solution for Efficient Energy Storage Applications. ACS Nano, 2019, 13, 9431-9441.	14.6	33
108	Accessing the Accuracy of Density Functional Theory through Structure and Dynamics of the Water–Air Interface. Journal of Physical Chemistry Letters, 2019, 10, 4914-4919.	4.6	43

#	Article	IF	CITATIONS
109	The Surface Activity of the Hydrated Proton Is Substantially Higher than That of the Hydroxide Ion. Angewandte Chemie - International Edition, 2019, 58, 15636-15639.	13.8	28
110	Quantitative Mapping of Triacylglycerol Chain Length and Saturation Using Broadband CARSÂMicroscopy. Biophysical Journal, 2019, 116, 2346-2355.	0.5	11
111	A semiconducting layered metal-organic framework magnet. Nature Communications, 2019, 10, 3260.	12.8	119
112	On the origin of the extremely different solubilities of polyethers in water. Nature Communications, 2019, 10, 2893.	12.8	88
113	Tunable Superstructures of Dendronized Graphene Nanoribbons in Liquid Phase. Journal of the American Chemical Society, 2019, 141, 10972-10977.	13.7	36
114	Unveiling Heterogeneity of Interfacial Water through the Water Bending Mode. Journal of Physical Chemistry Letters, 2019, 10, 6936-6941.	4.6	38
115	Das hydratisierte Proton besitzt eine deutlich höhere Oberflähenaktivitäals das Hydroxidion. Angewandte Chemie, 2019, 131, 15783-15786.	2.0	1
116	Control of Terahertz Nonlinearity in Graphene by Gating. , 2019, , .		0
117	Electrolytes Change the Interfacial Water Structure but Not the Vibrational Dynamics. Journal of Physical Chemistry B, 2019, 123, 8610-8616.	2.6	8
118	Surface-Specific Spectroscopy of Water at a Potentiostatically Controlled Supported Graphene Monolayer. Journal of Physical Chemistry C, 2019, 123, 24031-24038.	3.1	29
119	Unveiling Electronic Properties in Metal–Phthalocyanine-Based Pyrazine-Linked Conjugated Two-Dimensional Covalent Organic Frameworks. Journal of the American Chemical Society, 2019, 141, 16810-16816.	13.7	227
120	Unraveling the Origin of the Apparent Charge of Zwitterionic Lipid Layers. Journal of Physical Chemistry Letters, 2019, 10, 6355-6359.	4.6	17
121	Sun <i>etÂal.</i> Reply:. Physical Review Letters, 2019, 123, 099602.	7.8	1
122	Both Poly(ethylene glycol) and Poly(methyl ethylene phosphate) Guide Oriented Adsorption of Specific Proteins. Langmuir, 2019, 35, 14092-14097.	3.5	4
123	Molecular hydrophobicity at a macroscopically hydrophilic surface. Proceedings of the National Academy of Sciences of the United States of America, 2019, 116, 1520-1525.	7.1	109
124	The surface affinity of cations depends on both the cations and the nature of the surface. Journal of Chemical Physics, 2019, 150, 044706.	3.0	13
125	Automated cell segmentation in FIJI® using the DRAQ5 nuclear dye. BMC Bioinformatics, 2019, 20, 39.	2.6	14
126	Correlated interfacial water transport and proton conductivity in perfluorosulfonic acid membranes. Proceedings of the National Academy of Sciences of the United States of America, 2019, 116, 8715-8720.	7.1	39

#	Article	IF	CITATIONS
127	Peptide-Controlled Assembly of Macroscopic Calcium Oxalate Nanosheets. Journal of Physical Chemistry Letters, 2019, 10, 2170-2174.	4.6	18
128	Chemisorption of Atomically Precise 42-Carbon Graphene Quantum Dots on Metal Oxide Films Greatly Accelerates Interfacial Electron Transfer. Journal of Physical Chemistry Letters, 2019, 10, 1431-1436.	4.6	9
129	Phase-Sensitive Sum-Frequency Generation Measurements Using a Femtosecond Nonlinear Interferometer. Journal of Physical Chemistry C, 2019, 123, 7266-7270.	3.1	15
130	The Surface of Ice under Equilibrium and Nonequilibrium Conditions. Accounts of Chemical Research, 2019, 52, 1006-1015.	15.6	57
131	How water flips at charged titanium dioxide: an SFC-study on the water–TiO ₂ interface. Physical Chemistry Chemical Physics, 2019, 21, 8956-8964.	2.8	13
132	Dynamics of Dicyanamide in Ionic Liquids is Dominated by Local Interactions. Journal of Physical Chemistry B, 2019, 123, 1831-1839.	2.6	14
133	Vergleichende Acetonadsorption an Wasser―und Eisoberflähen. Angewandte Chemie, 2019, 131, 3659-3663.	2.0	0
134	How surface-specific is 2nd-order non-linear spectroscopy?. Journal of Chemical Physics, 2019, 151, 230901.	3.0	19
135	Kinetic Ionic Permeation and Interfacial Doping of Supported Graphene. Nano Letters, 2019, 19, 9029-9036.	9.1	16
136	Comparative Adsorption of Acetone on Water and Ice Surfaces. Angewandte Chemie - International Edition, 2019, 58, 3620-3624.	13.8	9
137	Specific Ion Effects on an Oligopeptide: Bidentate Binding Matters for the Guanidinium Cation. Angewandte Chemie - International Edition, 2019, 58, 332-337.	13.8	10
138	Spezifische Ionenâ€Effekte am Beispiel eines Oligopeptids: die Rolle zweizäniger Koordination beim Guanidiniumâ€Kation. Angewandte Chemie, 2019, 131, 338-343.	2.0	0
139	Hydration and Orientation of Carbonyl Groups in Oppositely Charged Lipid Monolayers on Water. Journal of Physical Chemistry B, 2019, 123, 1085-1089.	2.6	33
140	Interfacial Conformation of Hydrophilic Polyphosphoesters Affects Blood Protein Adsorption. ACS Applied Materials & Interfaces, 2019, 11, 1624-1629.	8.0	17
141	Two-Dimensional Terahertz-Infrared-Visible Spectroscopy Elucidates Coupling Between Low- and High-Frequency Modes. Springer Series in Optical Sciences, 2019, , 197-214.	0.7	2
142	Graphene: The Ultimate Nonlinear Material at Terahertz Frequencies. , 2019, , .		1
143	Reduced Near-Resonant Vibrational Coupling at the Surfaces of Liquid Water and Ice. Journal of Physical Chemistry Letters, 2018, 9, 1290-1294.	4.6	21
144	Coupling between intra- and intermolecular motions in liquid water revealed by two-dimensional terahertz-infrared-visible spectroscopy. Nature Communications, 2018, 9, 885.	12.8	67

#	Article	IF	CITATIONS
145	Structure from Dynamics: Vibrational Dynamics of Interfacial Water as a Probe of Aqueous Heterogeneity. Journal of Physical Chemistry B, 2018, 122, 3667-3679.	2.6	47
146	Engineering Proteins at Interfaces: From Complementary Characterization to Material Surfaces with Designed Functions. Angewandte Chemie - International Edition, 2018, 57, 12626-12648.	13.8	40
147	Engineering von Proteinen an OberflÄ e hen: Von komplementÄ r er Charakterisierung zu MaterialoberflÄ e hen mit maÄŸgeschneiderten Funktionen. Angewandte Chemie, 2018, 130, 12806-12830.	2.0	3
148	Dynamical heterogeneities of rotational motion in room temperature ionic liquids evidenced by molecular dynamics simulations. Journal of Chemical Physics, 2018, 148, 193811.	3.0	15
149	Time-Resolved Sum Frequency Generation Spectroscopy: A Quantitative Comparison Between Intensity and Phase-Resolved Spectroscopy. Journal of Physical Chemistry A, 2018, 122, 2401-2410.	2.5	19
150	Calcium-Induced Molecular Rearrangement of Peptide Folds Enables Biomineralization of Vaterite Calcium Carbonate. Journal of the American Chemical Society, 2018, 140, 2793-2796.	13.7	46
151	Saturation of charge-induced water alignment at model membrane surfaces. Science Advances, 2018, 4, eaap7415.	10.3	76
152	Out-of-plane heat transfer in van der Waals stacks through electron–hyperbolic phonon coupling. Nature Nanotechnology, 2018, 13, 41-46.	31.5	128
153	Genetically encoded lipid–polypeptide hybrid biomaterials that exhibit temperature-triggered hierarchical self-assembly. Nature Chemistry, 2018, 10, 496-505.	13.6	79
154	Definition of Free O–H Groups of Water at the Air–Water Interface. Journal of Chemical Theory and Computation, 2018, 14, 357-364.	5.3	46
155	Intense THz-assisted modulation of semiconductor optical properties. , 2018, , .		0
156	Orientational Distribution of Free O-H Groups of Interfacial Water is Exponential. Physical Review Letters, 2018, 121, 246101.	7.8	49
157	Counteracting Interfacial Energetics for Wetting of Hydrophobic Surfaces in the Presence of Surfactants. Langmuir, 2018, 34, 12344-12349.	3.5	19
158	Dynamics of Water Molecules at the Water/Air Interface. , 2018, , 348-355.		1
159	lce Nucleation at the Water–Sapphire Interface: Transient Sum-Frequency Response without Evidence for Transient Ice Phase. Journal of Physical Chemistry C, 2018, 122, 24760-24764.	3.1	10
160	High-mobility band-like charge transport in a semiconducting two-dimensional metal–organic framework. Nature Materials, 2018, 17, 1027-1032.	27.5	341
161	Surface Potential of a Planar Charged Lipid–Water Interface. What Do Vibrating Plate Methods, Second Harmonic and Sum Frequency Measure?. Journal of Physical Chemistry Letters, 2018, 9, 5685-5691.	4.6	44
162	Large Hydrogen-Bond Mismatch between TMAO and Urea Promotes Their Hydrophobic Association. CheM, 2018, 4, 2615-2627.	11.7	27

#	Article	IF	CITATIONS
163	Extremely efficient terahertz high-harmonic generation in graphene by hot Dirac fermions. Nature, 2018, 561, 507-511.	27.8	365
164	Resolution along both infrared and visible frequency axes in second-order Fourier-transform vibrational sum-frequency generation spectroscopy. Chemical Physics, 2018, 512, 27-35.	1.9	0
165	Quantifying Polaron Formation and Charge Carrier Cooling in Leadâ€lodide Perovskites. Advanced Materials, 2018, 30, e1707312.	21.0	124
166	Accurate terahertz spectroscopy of supported thin films by precise substrate thickness correction. Optics Letters, 2018, 43, 447.	3.3	22
167	Efficient Hot Electron Transfer in Quantum Dot-Sensitized Mesoporous Oxides at Room Temperature. Nano Letters, 2018, 18, 5111-5115.	9.1	21
168	The ultrafast dynamics and conductivity of photoexcited graphene at different Fermi energies. Science Advances, 2018, 4, eaar5313.	10.3	95
169	Molecular Insight into the Slipperiness of Ice. Journal of Physical Chemistry Letters, 2018, 9, 2838-2842.	4.6	63
170	Kopplung von hoch―und niederfrequenten Schwingungsmoden in organischâ€anorganischen Perowskiten. Angewandte Chemie, 2018, 130, 13845-13849.	2.0	0
171	Vibrational Coupling between Organic and Inorganic Sublattices of Hybrid Perovskites. Angewandte Chemie - International Edition, 2018, 57, 13657-13661.	13.8	34
172	Advanced Vibrational Spectroscopies, dedicated to Dr. Edwin J. Heilweil on the occasion of his 60th birthday. Chemical Physics, 2018, 512, 1-2.	1.9	0
173	Evidence for auto-catalytic mineral dissolution from surface-specific vibrational spectroscopy. Nature Communications, 2018, 9, 3316.	12.8	34
174	Reversible Photochemical Control of Doping Levels in Supported Graphene. Journal of Physical Chemistry C, 2017, 121, 4083-4091.	3.1	28
175	Trimethylamine- <i>N</i> -oxide: its hydration structure, surface activity, and biological function, viewed by vibrational spectroscopy and molecular dynamics simulations. Physical Chemistry Chemical Physics, 2017, 19, 6909-6920.	2.8	39
176	Acetylation dictates the morphology of nanophase biosilica precipitated by a 14â€amino acid leucine–lysine peptide. Journal of Peptide Science, 2017, 23, 141-147.	1.4	11
177	Chemical Vapor Deposition Synthesis and Terahertz Photoconductivity of Low-Band-Gap <i>N</i> = 9 Armchair Graphene Nanoribbons. Journal of the American Chemical Society, 2017, 139, 3635-3638.	13.7	88
178	Coordination Polymer Framework Based Onâ€Chip Microâ€Supercapacitors with AC Lineâ€Filtering Performance. Angewandte Chemie, 2017, 129, 3978-3982.	2.0	22
179	Coordination Polymer Framework Based On hip Micro‧upercapacitors with AC Lineâ€Filtering Performance. Angewandte Chemie - International Edition, 2017, 56, 3920-3924.	13.8	140
180	Nitrated Fatty Acids Modulate the Physical Properties of Model Membranes and the Structure of Transmembrane Proteins. Chemistry - A European Journal, 2017, 23, 9690-9697.	3.3	17

#	Article	IF	CITATIONS
181	Trap-Free Hot Carrier Relaxation in Lead–Halide Perovskite Films. Journal of Physical Chemistry C, 2017, 121, 11201-11206.	3.1	43
182	Single-crystal <i>I</i> _{<i>h</i>} ice surfaces unveil connection between macroscopic and molecular structure. Proceedings of the National Academy of Sciences of the United States of America, 2017, 114, 5349-5354.	7.1	12
183	Chemisorbed and Physisorbed Water at the TiO ₂ /Water Interface. Journal of Physical Chemistry Letters, 2017, 8, 2195-2199.	4.6	89
184	The Structure of the Diatom Silaffin Peptide R5 within Freestanding Twoâ€Dimensional Biosilica Sheets. Angewandte Chemie - International Edition, 2017, 56, 8277-8280.	13.8	34
185	Role of Edge Engineering in Photoconductivity of Graphene Nanoribbons. Journal of the American Chemical Society, 2017, 139, 7982-7988.	13.7	64
186	Conical Ionic Amphiphiles Endowed with Micellization Ability but Lacking Air–Water and Oil–Water Interfacial Activity. Journal of the American Chemical Society, 2017, 139, 7677-7680.	13.7	19
187	Thiolated Lysineâ€Leucine Peptides Selfâ€Assemble into Biosilica Nucleation Pits on Gold Surfaces. Advanced Materials Interfaces, 2017, 4, 1700399.	3.7	3
188	Correlating Carrier Dynamics and Photocatalytic Hydrogen Generation in Pt Decorated CdSe Tetrapods as a Function of Cocatalyst Size. Journal of Physical Chemistry C, 2017, 121, 13070-13077.	3.1	13
189	Boosting Biexciton Collection Efficiency at Quantum Dot–Oxide Interfaces by Hole Localization at the Quantum Dot Shell. Journal of Physical Chemistry Letters, 2017, 8, 2654-2658.	4.6	5
190	Determination of Absolute Orientation of Protein α-Helices at Interfaces Using Phase-Resolved Sum Frequency Generation Spectroscopy. Journal of Physical Chemistry Letters, 2017, 8, 3101-3105.	4.6	27
191	Femtosecond-timescale buildup of electron mobility in GaAs observed via ultrabroadband transient terahertz spectroscopy. Applied Physics Letters, 2017, 110, .	3.3	8
192	Anionic and cationic Hofmeister effects are non-additive for guanidinium salts. Physical Chemistry Chemical Physics, 2017, 19, 9724-9728.	2.8	11
193	Nanoparticle amount, and not size, determines chain alignment and nonlinear hardening in polymer nanocomposites. Proceedings of the National Academy of Sciences of the United States of America, 2017, 114, E3170-E3177.	7.1	24
194	Dipolar Molecular Capping in Quantum Dot-Sensitized Oxides: Fermi Level Pinning Precludes Tuning Donor–Acceptor Energetics. ACS Nano, 2017, 11, 4760-4767.	14.6	9
195	Ultraâ€Narrow Lowâ€Bandgap Graphene Nanoribbons from Bromoperylenes—Synthesis and Terahertz‧pectroscopy. Chemistry - A European Journal, 2017, 23, 4870-4875.	3.3	28
196	π ⁺ –π ⁺ stacking of imidazolium cations enhances molecular layering of room temperature ionic liquids at their interfaces. Physical Chemistry Chemical Physics, 2017, 19, 2850-2856.	2.8	42
197	Experimental and theoretical evidence for bilayer-by-bilayer surface melting of crystalline ice. Proceedings of the National Academy of Sciences of the United States of America, 2017, 114, 227-232.	7.1	131
198	LK peptide side chain dynamics at interfaces are independent of secondary structure. Physical Chemistry Chemical Physics, 2017, 19, 28507-28511.	2.8	13

#	Article	IF	CITATIONS
199	Role of Dielectric Drag in Polaron Mobility in Lead Halide Perovskites. ACS Energy Letters, 2017, 2, 2555-2562.	17.4	90
200	Direct observation of mode-specific phonon-band gap coupling in methylammonium lead halide perovskites. Nature Communications, 2017, 8, 687.	12.8	63
201	Excess Hydrogen Bond at the Ice-Vapor Interface around 200ÂK. Physical Review Letters, 2017, 119, 133003.	7.8	45
202	Repelling and ordering: the influence of poly(ethylene glycol) on protein adsorption. Physical Chemistry Chemical Physics, 2017, 19, 28182-28188.	2.8	36
203	Picosecond orientational dynamics of water in living cells. Nature Communications, 2017, 8, 904.	12.8	57
204	Measuring Intracellular Secondary Structure of a Cell-Penetrating Peptide in Situ. Analytical Chemistry, 2017, 89, 11310-11317.	6.5	11
205	Large area conductive nanoaperture arrays with strong optical resonances and spectrally flat terahertz transmission. Applied Physics Letters, 2017, 111, .	3.3	3
206	Electron Transfer from Bi-Isonicotinic Acid Emerges upon Photodegradation of N3-Sensitized TiO ₂ Electrodes. ACS Applied Materials & Interfaces, 2017, 9, 35376-35382.	8.0	5
207	Observation and Identification of a New OH Stretch Vibrational Band at the Surface of Ice. Journal of Physical Chemistry Letters, 2017, 8, 3656-3660.	4.6	53
208	Combining Time-of-Flight Secondary Ion Mass Spectrometry Imaging Mass Spectrometry and CARS Microspectroscopy Reveals Lipid Patterns Reminiscent of Gene Expression Patterns in the Wing Imaginal Disc of <i>Drosophila melanogaster</i> . Analytical Chemistry, 2017, 89, 9664-9670.	6.5	11
209	Surface-specific vibrational spectroscopy of the water/silica interface: screening and interference. Physical Chemistry Chemical Physics, 2017, 19, 16875-16880.	2.8	91
210	Die Struktur des Silaffinâ€Peptids R5 aus Diatomeen in freistehenden zweidimensionalen Biosilikatwäden. Angewandte Chemie, 2017, 129, 8390-8394.	2.0	2
211	Hydrogen bonding and vibrational energy relaxation of interfacial water: A full DFT molecular dynamics simulation. Journal of Chemical Physics, 2017, 147, 044707.	3.0	20
212	Photoswitchable Micro-Supercapacitor Based on a Diarylethene-Graphene Composite Film. Journal of the American Chemical Society, 2017, 139, 9443-9446.	13.7	96
213	Lateral Fusion of Chemical Vapor Deposited <i>N</i> = 5 Armchair Graphene Nanoribbons. Journal of the American Chemical Society, 2017, 139, 9483-9486.	13.7	65
214	Surface-charge-induced orientation of interfacial water suppresses heterogeneous ice nucleation on <i>α</i> -alumina (0001). Atmospheric Chemistry and Physics, 2017, 17, 7827-7837.	4.9	52
215	Sulfurâ€Enriched Conjugated Polymer Nanosheet Derived Sulfur and Nitrogen coâ€Đoped Porous Carbon Nanosheets as Electrocatalysts for Oxygen Reduction Reaction and Zinc–Air Battery. Advanced Functional Materials, 2016, 26, 5893-5902.	14.9	214
216	Hofmeisterâ€Effekte unter der Lupe: Die direkte Anionâ€Amidâ€Bindung ist schwÃ e her als die Kationâ€Amidâ€Bindung. Angewandte Chemie, 2016, 128, 8257-8261.	2.0	5

#	Article	IF	CITATIONS
217	Dissecting Hofmeister Effects: Direct Anion–Amide Interactions Are Weaker than Cation–Amide Binding. Angewandte Chemie - International Edition, 2016, 55, 8125-8128.	13.8	38
218	Nanoscale Distribution of Sulfonic Acid Groups Determines Structure and Binding of Water in Nafion Membranes. Angewandte Chemie, 2016, 128, 4079-4083.	2.0	7
219	Microscale spatial heterogeneity of protein structural transitions in fibrin matrices. Science Advances, 2016, 2, e1501778.	10.3	38
220	A new force field including charge directionality for TMAO in aqueous solution. Journal of Chemical Physics, 2016, 145, 064103.	3.0	7
221	Thermodynamic picture of terahertz conduction in graphene. , 2016, , .		Ο
222	Spin-resolved terahertz spectroscopy. , 2016, , .		0
223	Label-free <i>in situ</i> imaging of oil body dynamics and chemistry in germination. Journal of the Royal Society Interface, 2016, 13, 20160677.	3.4	14
224	Water orientation and hydrogen-bond structure at the fluorite/water interface. Scientific Reports, 2016, 6, 24287.	3.3	101
225	Surface tension of ab initio liquid water at the water-air interface. Journal of Chemical Physics, 2016, 144, 204705.	3.0	39
226	Enhanced Kinetics of Hole Transfer and Electrocatalysis during Photocatalytic Oxygen Evolution by Cocatalyst Tuning. ACS Catalysis, 2016, 6, 4117-4126.	11.2	48
227	Probing the charge separation process on In 2 S 3 /Pt-TiO 2 nanocomposites for boosted visible-light photocatalytic hydrogen production. Applied Catalysis B: Environmental, 2016, 198, 25-31.	20.2	56
228	Vibrational Spectroscopy and Dynamics of Water. Chemical Reviews, 2016, 116, 7590-7607.	47.7	300
229	Ultrafast Reorientational Dynamics of Leucine at the Air–Water Interface. Journal of the American Chemical Society, 2016, 138, 5226-5229.	13.7	26
230	Multimodal Spectroscopic Study of Amyloid Fibril Polymorphism. Journal of Physical Chemistry B, 2016, 120, 8809-8817.	2.6	30
231	Molecular Dynamics Simulations of SFG Librational Modes Spectra of Water at the Water–Air Interface. Journal of Physical Chemistry C, 2016, 120, 18665-18673.	3.1	34
232	Unveiling the Amphiphilic Nature of TMAO by Vibrational Sum Frequency Generation Spectroscopy. Journal of Physical Chemistry C, 2016, 120, 17435-17443.	3.1	33
233	Self-referenced ultra-broadband transient terahertz spectroscopy using air-photonics. Optics Express, 2016, 24, 10157.	3.4	8
234	Water in Contact with a Cationic Lipid Exhibits Bulklike Vibrational Dynamics. Journal of Physical Chemistry B, 2016, 120, 10069-10078.	2.6	26

#	Article	IF	CITATIONS
235	Comment on "Enhancement of Second-Order Nonlinear-Optical Signals by Optical Stimulation― Physical Review Letters, 2016, 116, 059401.	7.8	1
236	Both Inter- and Intramolecular Coupling of O–H Groups Determine the Vibrational Response of the Water/Air Interface. Journal of Physical Chemistry Letters, 2016, 7, 4591-4595.	4.6	101
237	lce-nucleating bacteria control the order and dynamics of interfacial water. Science Advances, 2016, 2, e1501630.	10.3	182
238	Nanoscale Distribution of Sulfonic Acid Groups Determines Structure and Binding of Water in Nafion Membranes. Angewandte Chemie - International Edition, 2016, 55, 4011-4015.	13.8	44
239	SAP(E) – A cell-penetrating polyproline helix at lipid interfaces. Biochimica Et Biophysica Acta - Biomembranes, 2016, 1858, 2028-2034.	2.6	29
240	Molecular Modeling of Water Interfaces: From Molecular Spectroscopy to Thermodynamics. Journal of Physical Chemistry B, 2016, 120, 3785-3796.	2.6	39
241	Oppositely Charged Ions at Water–Air and Water–Oil Interfaces: Contrasting the Molecular Picture with Thermodynamics. Journal of Physical Chemistry Letters, 2016, 7, 825-830.	4.6	29
242	Multiscale Self-Assembly of Silicon Quantum Dots into an Anisotropic Three-Dimensional Random Network. Nano Letters, 2016, 16, 1942-1948.	9.1	9
243	Hot electron transfer from PbSe quantum dots molecularly bridged to mesoporous tin and titanium oxide films. Chemical Physics, 2016, 471, 54-58.	1.9	12
244	Terahertz Carrier Dynamics in Graphene Nanoribbons with Different Peripherial Functional Groups. , 2016, , .		0
245	Ionic Liquids: Not only Structurally but also Dynamically Heterogeneous. Angewandte Chemie - International Edition, 2015, 54, 687-690.	13.8	41
246	Amyloid Fibrils: Nanoscale Heterogeneity of the Molecular Structure of Individual hIAPP Amyloid Fibrils Revealed with Tipâ€Enhanced Raman Spectroscopy (Small 33/2015). Small, 2015, 11, 4130-4130.	10.0	0
247	Efficient formation of excitons in a dense electron-hole plasma at room temperature. Physical Review B, 2015, 92, .	3.2	31
248	Molecular Mechanism of Water Evaporation. Physical Review Letters, 2015, 115, 236102.	7.8	75
249	Toward <i>ab initio</i> molecular dynamics modeling for sum-frequency generation spectra; an efficient algorithm based on surface-specific velocity-velocity correlation function. Journal of Chemical Physics, 2015, 143, 124702.	3.0	100
250	Nanoscale Heterogeneity of the Molecular Structure of Individual hIAPP Amyloid Fibrils Revealed with Tipâ€Enhanced Raman Spectroscopy. Small, 2015, 11, 4131-4139.	10.0	69
251	Molecular Structure and Dynamics of Water at the Water–Air Interface Studied with Surface‧pecific Vibrational Spectroscopy. Angewandte Chemie - International Edition, 2015, 54, 5560-5576.	13.8	132
252	Biomimetic Growth of Ultrathin Silica Sheets Using Artificial Amphiphilic Peptides. Advanced Materials Interfaces, 2015, 2, 1500282.	3.7	33

#	Article	IF	CITATIONS
253	Bovine and human insulin adsorption at lipid monolayers: a comparison. Frontiers in Physics, 2015, 3, .	2.1	13
254	Full membrane spanning self-assembled monolayers as model systems for UHV-based studies of cell-penetrating peptides. Biointerphases, 2015, 10, 019009.	1.6	6
255	Background-Free Fourth-Order Sum Frequency Generation Spectroscopy. Journal of Physical Chemistry Letters, 2015, 6, 2114-2120.	4.6	13
256	Perspective on terahertz spectroscopy of graphene. Europhysics Letters, 2015, 111, 67001.	2.0	31
257	Perilipin 5 mediated lipid droplet remodelling revealed by coherent Raman imaging. Integrative Biology (United Kingdom), 2015, 7, 467-476.	1.3	27
258	Controlled Folding of Graphene: GraFold Printing. Nano Letters, 2015, 15, 857-863.	9.1	27
259	Hydrogen Bond Dynamics in Primary Alcohols: A Femtosecond Infrared Study. Journal of Physical Chemistry B, 2015, 119, 1558-1566.	2.6	28
260	Interaction of a Patterned Amphiphilic Polyphenylene Dendrimer with a Lipid Monolayer: Electrostatic Interactions Dominate. Langmuir, 2015, 31, 1980-1987.	3.5	16
261	Thermodynamic picture of ultrafast charge transport in graphene. Nature Communications, 2015, 6, 7655.	12.8	147
262	<i>Ab Initio</i> Liquid Water Dynamics in Aqueous TMAO Solution. Journal of Physical Chemistry B, 2015, 119, 10597-10606.	2.6	44
263	Accessing the fundamentals of magnetotransport in metals with terahertz probes. Nature Physics, 2015, 11, 761-766.	16.7	103
264	Ultrafast Vibrational Dynamics of Water Disentangled by Reverse Nonequilibrium <i>AbÂlnitio</i> Molecular Dynamics Simulations. Physical Review X, 2015, 5, .	8.9	31
265	IM30 triggers membrane fusion in cyanobacteria and chloroplasts. Nature Communications, 2015, 6, 7018.	12.8	97
266	Boosting Power Conversion Efficiencies of Quantum-Dot-Sensitized Solar Cells Beyond 8% by Recombination Control. Journal of the American Chemical Society, 2015, 137, 5602-5609.	13.7	367
267	Role of Ion-Pairs in BrÃ,nsted Acid Catalysis. ACS Catalysis, 2015, 5, 6630-6633.	11.2	21
268	Lipid Carbonyl Groups Terminate the Hydrogen Bond Network of Membrane-Bound Water. Journal of Physical Chemistry Letters, 2015, 6, 4499-4503.	4.6	74
269	Photovoltaic Polymer-Fullerene Blends: Terahertz Carrier Dynamics and Device Performance. , 2015, , .		0
270	Multiscale Effects of Interfacial Polymer Confinement in Silica Nanocomposites. Macromolecules, 2015, 48, 7929-7937.	4.8	20

#	Article	IF	CITATIONS
271	Quantifying transient interactions between amide groups and the guanidinium cation. Physical Chemistry Chemical Physics, 2015, 17, 28539-28543.	2.8	14
272	The surface roughness, but not the water molecular orientation varies with temperature at the water–air interface. Physical Chemistry Chemical Physics, 2015, 17, 23559-23564.	2.8	60
273	Reversible Activation of a Cell-Penetrating Peptide in a Membrane Environment. Journal of the American Chemical Society, 2015, 137, 12199-12202.	13.7	52
274	Biomimetic vaterite formation at surfaces structurally templated by oligo(glutamic acid) peptides. Chemical Communications, 2015, 51, 15902-15905.	4.1	21
275	Strong frequency dependence of vibrational relaxation in bulk and surface water reveals sub-picosecond structural heterogeneity. Nature Communications, 2015, 6, 8384.	12.8	132
276	Phonon–Electron Scattering Limits Free Charge Mobility in Methylammonium Lead Iodide Perovskites. Journal of Physical Chemistry Letters, 2015, 6, 4991-4996.	4.6	186
277	Two Types of Water at the Water–Surfactant Interface Revealed by Time-Resolved Vibrational Spectroscopy. Journal of the American Chemical Society, 2015, 137, 14912-14919.	13.7	58
278	Reversible activation of pH-sensitive cell penetrating peptides attached to gold surfaces. Chemical Communications, 2015, 51, 273-275.	4.1	14
279	Water-mediated interactions between trimethylamine-N-oxide and urea. Physical Chemistry Chemical Physics, 2015, 17, 298-306.	2.8	70
280	Self-referenced Transient THz Spectroscopy with ABCD Detection. , 2015, , .		1
281	Control of Energy Relaxation Pathways in Graphene: Carrier-Carrier Scattering vs Phonon Emission. , 2015, , .		0
282	Perilipin 5 mediated lipid droplet remodelling revealed by coherent Raman imaging. FASEB Journal, 2015, 29, 568.19.	0.5	0
283	Ultra-broadband THz time-domain spectroscopy of common polymers using THz air photonics. Optics Express, 2014, 22, 12475.	3.4	121
284	Terahertz Carrier Dynamics in Graphene and Graphene Nanostructures. , 2014, , .		0
285	Inherent Resistivity of Graphene to Strong THz Fields. , 2014, , .		0
286	Nonlinear THz conductivity in graphene. , 2014, , .		0
287	Probing ultrafast temperature changes of aqueous solutions with coherent terahertz pulses. Optics Letters, 2014, 39, 1717.	3.3	14
288	Ultrafast carrier dynamics in graphene and graphene nanostructures. , 2014, , .		0

#	Article	IF	CITATIONS
289	Sticky water surfaces: Helix–coil transitions suppressed in a cell-penetrating peptide at the air-water interface. Journal of Chemical Physics, 2014, 141, 22D517.	3.0	24
290	Structural Basis for the Polymorphism of \hat{I}^2 -Lactoglobulin Amyloid-Like Fibrils. , 2014, , 333-343.		7
291	Polylactideâ€ <i>block</i> â€Polypeptideâ€ <i>block</i> â€Polylactide Copolymer Nanoparticles with Tunable Cleavage and Controlled Drug Release. Advanced Functional Materials, 2014, 24, 4026-4033.	14.9	33
292	Influence of surface polarity on water dynamics at the water/rutile TiO ₂ (110) interface. Journal of Physics Condensed Matter, 2014, 26, 244102.	1.8	30
293	Chemical imaging of lipid droplets in muscle tissues using hyperspectral coherent Raman microscopy. Histochemistry and Cell Biology, 2014, 141, 263-273.	1.7	35
294	Synthesis of structurally well-defined and liquid-phase-processable graphene nanoribbons. Nature Chemistry, 2014, 6, 126-132.	13.6	468
295	Label-free characterization of biomembranes: from structure to dynamics. Chemical Society Reviews, 2014, 43, 887-900.	38.1	72
296	Terahertz Depolarization Effects in Colloidal TiO ₂ Films Reveal Particle Morphology. Journal of Physical Chemistry C, 2014, 118, 1191-1197.	3.1	16
297	Quantifying Surfactant Alkyl Chain Orientation and Conformational Order from Sum Frequency Generation Spectra of CH Modes at the Surfactant–Water Interface. Journal of Physical Chemistry Letters, 2014, 5, 3737-3741.	4.6	34
298	Ultrafast Terahertz Photoconductivity of Photovoltaic Polymer–Fullerene Blends: A Comparative Study Correlated with Photovoltaic Device Performance. Journal of Physical Chemistry Letters, 2014, 5, 3662-3668.	4.6	52
299	Formation of Lysozyme Oligomers at Model Cell Membranes Monitored with Sum Frequency Generation Spectroscopy. Langmuir, 2014, 30, 7736-7744.	3.5	29
300	Bottom-Up Synthesis of Liquid-Phase-Processable Graphene Nanoribbons with Near-Infrared Absorption. ACS Nano, 2014, 8, 11622-11630.	14.6	138
301	Gigahertz Modulation of Femtosecond Time-Resolved Surface Sum-Frequency Generation Due to Acoustic Strain Pulses. Journal of Physical Chemistry C, 2014, 118, 20875-20880.	3.1	5
302	Observation of Water Separated Ion-Pairs between Cations and Phospholipid Headgroups. Journal of Physical Chemistry B, 2014, 118, 4397-4403.	2.6	18
303	Interplay Between Structure, Stoichiometry, and Electron Transfer Dynamics in SILAR-based Quantum Dot-Sensitized Oxides. Nano Letters, 2014, 14, 5780-5786.	9.1	26
304	Aqueous Heterogeneity at the Air/Water Interface Revealed by 2Dâ€HD‧FG Spectroscopy. Angewandte Chemie - International Edition, 2014, 53, 8146-8149.	13.8	106
305	Competing Ultrafast Energy Relaxation Pathways in Photoexcited Graphene. Nano Letters, 2014, 14, 5839-5845.	9.1	97
306	Hydration of Sodium Alginate in Aqueous Solution. Macromolecules, 2014, 47, 771-776.	4.8	45

#	Article	IF	CITATIONS
307	Liquid flow along a solid surface reversibly alters interfacial chemistry. Science, 2014, 344, 1138-1142.	12.6	187
308	Extreme surface propensity of halide ions in water. Nature Communications, 2014, 5, 4083.	12.8	97
309	Serotonergic innervation and serotonin receptor expression of NPY-producing neurons in the rat lateral and basolateral amygdaloid nuclei. Brain Structure and Function, 2013, 218, 421-435.	2.3	60
310	Density-dependent electron scattering in photoexcited GaAs in strongly diffusive regime. Applied Physics Letters, 2013, 102, 231120.	3.3	48
311	Unraveling the Link between Molecular Conformation and Morphology and Mechanics of Amyloid Fibrils. Biophysical Journal, 2013, 104, 553a-554a.	0.5	0
312	Folding and Unfolding of pH Sensitive Peptides: The Role of Interfaces. Biophysical Journal, 2013, 104, 394a.	0.5	0
313	Ultrafast Photoconductivity of Graphene Nanoribbons and Carbon Nanotubes. Nano Letters, 2013, 13, 5925-5930.	9.1	117
314	Coherent Anti-Stokes Raman Scattering Microspectroscopic Kinetic Study of Fast Hydrogen Bond Formation in Microfluidic Devices. Analytical Chemistry, 2013, 85, 8923-8927.	6.5	6
315	Tuning Electron Transfer Rates through Molecular Bridges in Quantum Dot Sensitized Oxides. Nano Letters, 2013, 13, 5311-5315.	9.1	83
316	Mechanism of vibrational energy dissipation of free OH groups at the air–water interface. Proceedings of the National Academy of Sciences of the United States of America, 2013, 110, 18780-18785.	7.1	77
317	Nonlinear terahertz conductivity in graphene. , 2013, , .		0
318	The Role of Intact Oleosin for Stabilization and Function of Oleosomes. Journal of Physical Chemistry B, 2013, 117, 13872-13883.	2.6	75
319	Photoexcitation cascade and multiple hot-carrier generation in graphene. Nature Physics, 2013, 9, 248-252.	16.7	512
320	Amyloids: From molecular structure to mechanical properties. Polymer, 2013, 54, 2473-2488.	3.8	89
321	Enhanced Autoionization of Water at Phospholipid Interfaces. Journal of Physical Chemistry C, 2013, 117, 510-514.	3.1	13
322	Water Bending Mode at the Water–Vapor Interface Probed by Sum-Frequency Generation Spectroscopy: A Combined Molecular Dynamics Simulation and Experimental Study. Journal of Physical Chemistry Letters, 2013, 4, 1872-1877.	4.6	100
323	Determining In Situ Protein Conformation and Orientation from the Amide-I Sum-Frequency Generation Spectrum: Theory and Experiment. Journal of Physical Chemistry A, 2013, 117, 6311-6322.	2.5	81
324	Single-pulse terahertz coherent control of spin resonance in the canted antiferromagnet YFeO <mml:math <br="" xmlns:mml="http://www.w3.org/1998/Math/MathML">display="inline"><mml:msub><mml:mrow></mml:mrow><mml:mn>3</mml:mn></mml:msub></mml:math> , mediated by dielectric anisotropy. Physical Review B, 2013, 87, .	3.2	74

#	Article	IF	CITATIONS
325	Structural Properties of gp41 Fusion Peptide at a Model Membrane Interface. Journal of Physical Chemistry B, 2013, 117, 15527-15535.	2.6	15
326	Biocompatible Polylactide-block-Polypeptide-block-Polylactide Nanocarrier. Biomacromolecules, 2013, 14, 1572-1577.	5.4	18
327	Near shot-noise limited hyperspectral stimulated Raman scattering spectroscopy using low energy lasers and a fast CMOS array. Optics Express, 2013, 21, 15113.	3.4	49
328	Photoexcitation cascade and multiple hot carrier generation in graphene. , 2013, , .		0
329	Hot carrier multiplication in graphene. , 2013, , .		0
330	Single-pulse terahertz coherent control of spin resonance in a canted antiferromagnet. , 2013, , .		0
331	Terahertz photoconductivity of graphene nanostructures. , 2013, , .		0
332	Density-dependent electron scattering in photoexcited GaAs. , 2013, , .		0
333	Ultrafast dynamics of water at the water-air interface studied by femtosecond surface vibrational spectroscopy. EPJ Web of Conferences, 2013, 41, 06009.	0.3	1
334	CHAPTER 11. Carrier Dynamics in Photovoltaic Structures and Materials Studied by Time-Resolved Terahertz Spectroscopy. RSC Energy and Environment Series, 2013, , 301-336.	0.5	1
335	Detection of deep-subwavelength dielectric layers at terahertz frequencies using semiconductor plasmonic resonators. Optics Express, 2012, 20, 5052.	3.4	41
336	Index mismatch aberration correction over long working distances using spatial light modulation. Applied Optics, 2012, 51, 8034.	1.8	9
337	Carrier multiplication in bulk indium nitride. Applied Physics Letters, 2012, 101, .	3.3	14
338	Nuclear Quantum Effects Affect Bond Orientation of Water at the Water-Vapor Interface. Physical Review Letters, 2012, 109, 226101.	7.8	79
339	Interfacial Water Facilitates Energy Transfer by Inducing Extended Vibrations in Membrane Lipids. Journal of Physical Chemistry B, 2012, 116, 6455-6460.	2.6	15
340	Assessing Charge Carrier Trapping in Silicon Nanowires Using Picosecond Conductivity Measurements. Nano Letters, 2012, 12, 3821-3827.	9.1	16
341	Hydration strongly affects the molecular and electronic structure of membrane phospholipids. Journal of Chemical Physics, 2012, 136, 114709.	3.0	48
342	Laser-Heating-Induced Displacement of Surfactants on the Water Surface. Journal of Physical Chemistry B, 2012, 116, 2703-2712.	2.6	60

#	Article	IF	CITATIONS
343	Loosening Quantum Confinement: Observation of Real Conductivity Caused by Hole Polarons in Semiconductor Nanocrystals Smaller than the Bohr Radius. Nano Letters, 2012, 12, 4937-4942.	9.1	16
344	Hydrogen-Bond Dynamics in a Protic Ionic Liquid: Evidence of Large-Angle Jumps. Journal of Physical Chemistry Letters, 2012, 3, 3034-3038.	4.6	65
345	The Polyphenol EGCG Inhibits Amyloid Formation Less Efficiently at Phospholipid Interfaces than in Bulk Solution. Journal of the American Chemical Society, 2012, 134, 14781-14788.	13.7	118
346	Hydration Dynamics of Hyaluronan and Dextran. Biophysical Journal, 2012, 103, L10-L12.	0.5	47
347	On the Role of Fresnel Factors in Sum-Frequency Generation Spectroscopy of Metal–Water and Metal-Oxide–Water Interfaces. Journal of Physical Chemistry C, 2012, 116, 23351-23361.	3.1	65
348	Tracing Catalytic Conversion on Single Zeolite Crystals in 3D with Nonlinear Spectromicroscopy. Journal of the American Chemical Society, 2012, 134, 1124-1129.	13.7	22
349	Complex Formation in Aqueous Trimethylamine- <i>N</i> -oxide (TMAO) Solutions. Journal of Physical Chemistry B, 2012, 116, 4783-4795.	2.6	127
350	Host–Guest Geometry in Pores of Zeolite ZSMâ€5 Spatially Resolved with Multiplex CARS Spectromicroscopy. Angewandte Chemie - International Edition, 2012, 51, 1343-1347.	13.8	27
351	No Ice-Like Water at Aqueous Biological Interfaces. Biointerphases, 2012, 7, 20.	1.6	39
352	Reversible Optical Control of Monolayers on Water through Photoswitchable Lipids. Journal of Physical Chemistry B, 2011, 115, 2294-2302.	2.6	32
353	Uptake of Gold Nanoparticles in Healthy and Tumor Cells Visualized by Nonlinear Optical Microscopy. Journal of Physical Chemistry B, 2011, 115, 5008-5016.	2.6	32
354	Comparative Study of Direct and Phase-Specific Vibrational Sum-Frequency Generation Spectroscopy: Advantages and Limitations. Journal of Physical Chemistry B, 2011, 115, 15362-15369.	2.6	73
355	Morphology and Persistence Length of Amyloid Fibrils Are Correlated to Peptide Molecular Structure. Journal of the American Chemical Society, 2011, 133, 18030-18033.	13.7	112
356	Anisotropic Water Reorientation around lons. Journal of Physical Chemistry B, 2011, 115, 12638-12647.	2.6	108
357	Ultrafast vibrational energy transfer at the water/air interface revealed by two-dimensional surface vibrational spectroscopy. Nature Chemistry, 2011, 3, 888-893.	13.6	177
358	Single substitutional nitrogen defects revealed as electron acceptor states in diamond using ultrafast spectroscopy. Physical Review B, 2011, 84, .	3.2	36
359	Serotonin transporter knockout and repeated social defeat stress: Impact on neuronal morphology and plasticity in limbic brain areas. Behavioural Brain Research, 2011, 220, 42-54.	2.2	43
360	Size-Dependent Electron Transfer from PbSe Quantum Dots to SnO2Monitored by Picosecond Terahertz Spectroscopy. Nano Letters, 2011, 11, 5234-5239.	9.1	53

#	Article	IF	CITATIONS
361	CARS microscopy for the visualization of micrometer-sized iron oxide MRI contrast agents in living cells. Biomedical Optics Express, 2011, 2, 2470.	2.9	8
362	Quantitative Coherent Anti-Stokes Raman Scattering (CARS) Microscopy. Journal of Physical Chemistry B, 2011, 115, 7713-7725.	2.6	120
363	Communication: Interfacial water structure revealed by ultrafast two-dimensional surface vibrational spectroscopy. Journal of Chemical Physics, 2011, 135, 021101.	3.0	47
364	Carrier dynamics in semiconductors studied with time-resolved terahertz spectroscopy. Reviews of Modern Physics, 2011, 83, 543-586.	45.6	978
365	Picosecond Electron Injection Dynamics in Dye-Sensitized Oxides in the Presence of Electrolyte. Journal of Physical Chemistry C, 2011, 115, 2578-2584.	3.1	63
366	Unified Molecular View of the Air/Water Interface Based on Experimental and Theoretical χ ⁽²⁾ Spectra of an Isotopically Diluted Water Surface. Journal of the American Chemical Society, 2011, 133, 16875-16880.	13.7	245
367	Anomalous Independence of Multiple Exciton Generation on Different Group IVâ^'VI Quantum Dot Architectures. Nano Letters, 2011, 11, 1623-1629.	9.1	61
368	Vibrational and orientational dynamics of water in aqueous hydroxide solutions. Journal of Chemical Physics, 2011, 135, 124517.	3.0	23
369	Ultrafast Reorientation of Dangling OH Groups at the Air-Water Interface Using Femtosecond Vibrational Spectroscopy. Physical Review Letters, 2011, 107, 116102.	7.8	84
370	Precision waveguide system for measurement of complex permittivity of liquids at frequencies from 60 to 90ÂGHz. Review of Scientific Instruments, 2011, 82, 104703.	1.3	7
371	Quantitative CARS Molecular Fingerprinting of Single Living Cells with the Use of the Maximum Entropy Method. Angewandte Chemie - International Edition, 2010, 49, 6773-6777.	13.8	97
372	Ultrafast surface vibrational dynamics. Surface Science Reports, 2010, 65, 45-66.	7.2	148
373	Time domain terahertz spectroscopy for investigating the dielectric relaxation dynamics of water in model membranes. , 2010, , .		0
374	Quantitative CARS Spectral Imaging of a Single Living Cell in the Fingerprint Region. , 2010, , .		0
375	Spectroscopic Studies of Electron Injection in Quantum Dot Sensitized Mesoporous Oxide Films. Journal of Physical Chemistry C, 2010, 114, 18866-18873.	3.1	47
376	Carrier multiplication in bulk and nanocrystalline semiconductors: Mechanism, efficiency, and interest for solar cells. Physical Review B, 2010, 81, .	3.2	80
377	(Multi)exciton Dynamics and Exciton Polarizability in Colloidal InAs Quantum Dots. Journal of Physical Chemistry C, 2010, 114, 6318-6324.	3.1	27
378	Duramycin-Induced Destabilization of a Phosphatidylethanolamine Monolayer at the Airâ^'Water Interface Observed by Vibrational Sum-Frequency Generation Spectroscopy. Langmuir, 2010, 26, 16055-16062.	3.5	33

#	Article	IF	CITATIONS
379	Molecular Restructuring of Water and Lipids upon the Interaction of DNA with Lipid Monolayers. Journal of the American Chemical Society, 2010, 132, 8037-8047.	13.7	40
380	Label-Free Imaging of Lipophilic Bioactive Molecules during Lipid Digestion by Multiplex Coherent Anti-Stokes Raman Scattering Microspectroscopy. Journal of the American Chemical Society, 2010, 132, 8433-8439.	13.7	74
381	Structural Inhomogeneity of Interfacial Water at Lipid Monolayers Revealed by Surface-Specific Vibrational Pumpâ ³⁹ Probe Spectroscopy. Journal of the American Chemical Society, 2010, 132, 14971-14978.	13.7	82
382	Influence of Concentration and Temperature on the Dynamics of Water in the Hydrophobic Hydration Shell of Tetramethylurea. Journal of the American Chemical Society, 2010, 132, 15671-15678.	13.7	124
383	Ultrafast active control of localized surface plasmon resonances in silicon bowtie antennas. Optics Express, 2010, 18, 23226.	3.4	70
384	Cooperativity in Ion Hydration. Science, 2010, 328, 1006-1009.	12.6	562
385	Surface Femtochemistry. , 2010, , 203-221.		1
386	Ultrafast inter- and intramolecular vibrational energy transfer between molecules at interfaces studied by time- and polarization-resolved SFG spectroscopy. Physical Chemistry Chemical Physics, 2010, 12, 12909.	2.8	22
387	TeraHertz Dielectric Relaxation of Biological Water Confined in Model Membranes made of Lyotropic Phospholipids. Molecular Crystals and Liquid Crystals, 2009, 500, 108-117.	0.9	11
388	Observation of buried water molecules in phospholipid membranes by surface sum-frequency generation spectroscopy. Journal of Chemical Physics, 2009, 131, 161107.	3.0	75
389	Imaging of chemical and physical state of individual cellular lipid droplets using multiplex CARS microscopy. Journal of Raman Spectroscopy, 2009, 40, 763-769.	2.5	35
390	Labelâ€Free Chemical Imaging of Catalytic Solids by Coherent Antiâ€Stokes Raman Scattering and Synchrotronâ€Based Infrared Microscopy. Angewandte Chemie - International Edition, 2009, 48, 8990-8994.	13.8	65
391	Optical methods for the study of dynamics in biological membrane models. Surface Science, 2009, 603, 1945-1952.	1.9	11
392	Assessment of carrier-multiplication efficiency in bulk PbSe and PbS. Nature Physics, 2009, 5, 811-814.	16.7	245
393	Hydrogen bonding strength of interfacial water determined with surface sum-frequency generation. Chemical Physics Letters, 2009, 470, 7-12.	2.6	137
394	Observation of photoactive yellow protein anchored to a modified Au(1 1 1) surface by scanning tunneling microscopy. Chemical Physics Letters, 2009, 472, 113-117.	2.6	7
395	Determining Absolute Molecular Orientation at Interfaces: A Phase Retrieval Approach for Sum Frequency Generation Spectroscopy. Journal of Physical Chemistry C, 2009, 113, 6100-6106.	3.1	82
396	Suppression of Proton Mobility by Hydrophobic Hydration. Journal of the American Chemical Society, 2009, 131, 17070-17071.	13.7	27

#	Article	IF	CITATIONS
397	Measuring Molecular Reorientation at Liquid Surfaces with Time-Resolved Sum-Frequency Spectroscopy: A Theoretical Framework. Journal of Physical Chemistry B, 2009, 113, 7564-7573.	2.6	30
398	Interface-Specific Ultrafast Two-Dimensional Vibrational Spectroscopy. Accounts of Chemical Research, 2009, 42, 1332-1342.	15.6	89
399	Coherent anti-Stokes Raman scattering microscopy for quantitative characterization of mixing and flow in microfluidics. Optics Letters, 2009, 34, 211.	3.3	14
400	Dielectric Relaxation Dynamics of Water in Model Membranes Probed by Terahertz Spectroscopy. Biophysical Journal, 2009, 97, 2484-2492.	0.5	166
401	Structure Dynamics of the Proton in Liquid Water Probed with Terahertz Time-Domain Spectroscopy. Physical Review Letters, 2009, 102, 198303.	7.8	91
402	Structure and dynamics of interfacial water in model lung surfactants. Faraday Discussions, 2009, 141, 145-159.	3.2	18
403	Ultrafast 2D-IR spectroscopy of a molecular monolayer. Springer Series in Chemical Physics, 2009, , 511-513.	0.2	0
404	THz Studies of Charge and Exciton Dynamics in Semiconductor Nanostructures. , 2009, , .		0
405	Ultrafast vibrational dynamics of interfacial water. Springer Series in Chemical Physics, 2009, , 517-519.	0.2	0
406	Ultrafast vibrational dynamics of interfacial water. Chemical Physics, 2008, 350, 23-30.	1.9	27
407	Label-free cellular imaging of lipid composition of individual lipid droplets using multiplex CARS microscopy. Chemistry and Physics of Lipids, 2008, 154, S5.	3.2	2
408	Sum-frequency generation spectroscopy of self-assembled structures of Guanosine 5′-monophosphate on mica. Chemical Physics Letters, 2008, 467, 159-163.	2.6	3
409	In Situ Quantitative Measurement of Concentration Profiles in a Microreactor with Submicron Resolution Using Multiplex CARS Microscopy. Journal of the American Chemical Society, 2008, 130, 11592-11593.	13.7	47
410	Quantitative Label-Free Imaging of Lipid Composition and Packing of Individual Cellular Lipid Droplets Using Multiplex CARS Microscopy. Biophysical Journal, 2008, 95, 4908-4914.	0.5	205
411	Vibrational Response of Hydrogen-Bonded Interfacial Water is Dominated by Intramolecular Coupling. Physical Review Letters, 2008, 100, 173901.	7.8	296
412	A THz spectrometer based on a CsI prism. Journal of Optics, 2008, 10, 095303.	1.5	6
413	On the mechanism of charge transport in pentacene. Journal of Chemical Physics, 2008, 129, 044704.	3.0	46
414	Optical Control over Surface-Plasmon-Polariton-Assisted THz Transmission through a Slit Aperture. Physical Review Letters, 2008, 100, 123901.	7.8	125

#	Article	IF	CITATIONS
415	Photoinduced charge-carriers in SrTiO <inf>3</inf> crystals investigated by pump-probe THz spectroscopy. , 2008, , .		0
416	On the Absence of Detectable Carrier Multiplication in a Transient Absorption Study of InAs/CdSe/ZnSe Core/Shell1/Shell2 Quantum Dots. Nano Letters, 2008, 8, 1207-1211.	9.1	159
417	On the Wavelength-Dependent Performance of Cr-Doped Silica in Selective Photo-Oxidation. Journal of Physical Chemistry C, 2008, 112, 5471-5475.	3.1	14
418	Ultrafast Two Dimensional-Infrared Spectroscopy of a Molecular Monolayer. Journal of the American Chemical Society, 2008, 130, 2152-2153.	13.7	95
419	Liquid Crystal Colloids Studied by THz Time-Domain Spectroscopy. Molecular Crystals and Liquid Crystals, 2008, 480, 21-28.	0.9	3
420	Femtosecond time-resolved and two-dimensional vibrational sum frequency spectroscopic instrumentation to study structural dynamics at interfaces. Review of Scientific Instruments, 2008, 79, 093907.	1.3	36
421	Sovagoet al.Reply:. Physical Review Letters, 2008, 101, .	7.8	32
422	Coherent Anti-Stokes Raman Scattering (CARS) microscopy for three-dimensional flow characterization in microfluidics. , 2008, , .		0
423	Ultrafast intraband relaxation in colloidal quantum dots. , 2008, , .		0
424	Retrieving the susceptibility from time-resolved terahertz experiments. Journal of Chemical Physics, 2007, 127, 094308.	3.0	7
425	Deposition and crystallization studies of thin amorphous solid water films on Ru(0001) and on CO-precovered Ru(0001). Journal of Chemical Physics, 2007, 127, 094703.	3.0	42
426	Ultrafast energy flow in model biological membranes. New Journal of Physics, 2007, 9, 390-390.	2.9	51
427	Morphological change during crystallization of thin amorphous solid water films on Ru(0001). Journal of Chemical Physics, 2007, 126, 181103.	3.0	29
428	Simultaneous ultrafast probing of intramolecular vibrations and photoinduced charge carriers in rubrene using broadband time-domain THz spectroscopy. Physical Review B, 2007, 75, .	3.2	15
429	Ultrafast optical switching of the THz transmission through metallic subwavelength hole arrays. Physical Review B, 2007, 75, .	3.2	80
430	Ultrafast Vibrational Energy Transfer between Surface and Bulk Water at the Air-Water Interface. Physical Review Letters, 2007, 98, 098302.	7.8	102
431	Reduction of carrier mobility in semiconductors caused by charge-charge interactions. Physical Review B, 2007, 75, .	3.2	55

432 THz time-domain spectroscopy of liquid crystal colloids. , 2007, , .

#	Article	IF	CITATIONS
433	Multiplex coherent anti-Stokes Raman scattering microscopy on lipid droplets in HeLa cells. Proceedings of SPIE, 2007, , .	0.8	0
434	Quantitative multiplex CARS spectroscopy in congested spectral regions. , 2007, , .		2
435	Ultrafast Electron-Induced Desorption of Water from Nanometer Amorphous Solid Water Films. Journal of Physical Chemistry B, 2007, 111, 6141-6145.	2.6	10
436	Sensitive Probing of DNA Binding to a Cationic Lipid Monolayer. Journal of the American Chemical Society, 2007, 129, 8420-8421.	13.7	68
437	Polarization-Resolved Broad-Bandwidth Sum-Frequency Generation Spectroscopy of Monolayer Relaxationâ€. Journal of Physical Chemistry C, 2007, 111, 8878-8883.	3.1	33
438	Highly Efficient Ultrafast Energy Transfer into Molecules at Surface Step Sites. Journal of Physical Chemistry C, 2007, 111, 6149-6153.	3.1	16
439	Membrane-Bound Water is Energetically Decoupled from Nearby Bulk Water:  An Ultrafast Surface-Specific Investigation. Journal of the American Chemical Society, 2007, 129, 9608-9609.	13.7	83
440	Carrier Multiplication and Its Reduction by Photodoping in Colloidal InAs Quantum Dots. Journal of Physical Chemistry C, 2007, 111, 4146-4152.	3.1	172
441	Calcium-Induced Phospholipid Ordering Depends on Surface Pressure. Journal of the American Chemical Society, 2007, 129, 11079-11084.	13.7	110
442	Quantitative CARS Spectroscopy Using the Maximum Entropy Method: The Main Lipid Phase Transition. ChemPhysChem, 2007, 8, 279-287.	2.1	86
443	THz dielectric relaxation of ionic liquid:water mixtures. Chemical Physics Letters, 2007, 439, 60-64.	2.6	95
444	The distinct vibrational signature of grain-boundary water in nano-crystalline ice films. Chemical Physics Letters, 2007, 448, 121-126.	2.6	9
445	Direct measurement of phase coexistence in DPPC/cholesterol vesicles using Raman spectroscopy. Chemistry and Physics of Lipids, 2007, 146, 76-84.	3.2	43
446	Exciton and electron-hole plasma formation dynamics in ZnO. Physical Review B, 2007, 76, .	3.2	77
447	Quantitative Multiplex CARS Spectroscopy in Congested Spectral Regions. Journal of Physical Chemistry B, 2006, 110, 4472-4479.	2.6	64
448	Direct Observation of Electron-to-Hole Energy Transfer in CdSe Quantum Dots. Physical Review Letters, 2006, 96, 057408.	7.8	197
449	Surface molecular view of colloidal gelation. Proceedings of the National Academy of Sciences of the United States of America, 2006, 103, 13310-13314.	7.1	57
450	Direct extraction of Raman line-shapes from congested CARS spectra. Optics Express, 2006, 14, 3622.	3.4	210

#	Article	IF	CITATIONS
451	High-frequency dielectric relaxation of liquid crystals: THz time-domain spectroscopy of liquid crystal colloids. Optics Express, 2006, 14, 11433.	3.4	23
452	Exciton polarizability in semiconductor nanocrystals. Nature Materials, 2006, 5, 861-864.	27.5	146
453	Free carrier photogeneration in polythiophene versus poly(phenylene vinylene) studied with THz spectroscopy. Chemical Physics Letters, 2006, 432, 441-445.	2.6	44
454	Adsorption and photochemistry of multilayer bromoform on ice. Surface Science, 2006, 600, 3337-3344.	1.9	6
455	Local Field Effects on Electron Transport in Nanostructured TiO2 Revealed by Terahertz Spectroscopy. Nano Letters, 2006, 6, 755-759.	9.1	351
456	Spectroscopic analysis of the oxygenation state of hemoglobin using coherent anti-Stokes Raman scattering. Journal of Biomedical Optics, 2006, 11, 050502.	2.6	28
457	A quantitative comparison between reflection absorption infrared and sum-frequency generation spectroscopy. Chemical Physics Letters, 2005, 412, 152-157.	2.6	22
458	The CO–H interaction on Pt(1 1 1) studied using temperature programmed vibrational sum frequency generation. Chemical Physics Letters, 2005, 412, 482-487.	2.6	3
459	Femtosecond sum frequency generation at the metal–liquid interface. Surface Science, 2005, 593, 79-88.	1.9	25
460	Interface–solvent effects during colloidal phase transitions. Journal of Physics Condensed Matter, 2005, 17, S3469-S3479.	1.8	31
461	Interchain effects in the ultrafast photophysics of a semiconducting polymer:THztime-domain spectroscopy of thin films and isolated chains in solution. Physical Review B, 2005, 71, .	3.2	110
462	Simulation studies of pore and domain formation in a phospholipid monolayer. Journal of Chemical Physics, 2005, 122, 024704.	3.0	54
463	Surface Photochemistry of Bromoform on Ice:Â Cross Section and Competing Reaction Pathways. Journal of Physical Chemistry B, 2005, 109, 17574-17578.	2.6	8
464	Theory of sum-frequency generation spectroscopy of adsorbed molecules using the density matrix method—broadband vibrational sum-frequency generation and applications. Journal of Physics Condensed Matter, 2005, 17, S201-S220.	1.8	20
465	Real-Time Observation of Molecular Motion on a Surface. Science, 2005, 310, 1790-1793.	12.6	167
466	Ultrafast scattering of electrons in TiO2. , 2004, , 517-520.		3
467	Surface Crystallization of Amorphous Solid Water. Physical Review Letters, 2004, 92, 236101.	7.8	81
468	Adsorption and dissociation of NO on stepped Pt (533). Journal of Chemical Physics, 2004, 121, 7946.	3.0	44

#	Article	IF	CITATIONS
469	Efficiency of Exciton and Charge Carrier Photogeneration in a Semiconducting Polymer. Physical Review Letters, 2004, 92, 196601.	7.8	183
470	Nonlinear optical scattering: The concept of effective susceptibility. Physical Review B, 2004, 70, .	3.2	150
471	Comment on "Ultrafast Laser Excitation ofCO/Pt(111)Probed by Sum Frequency Generation: Coverage Dependent Desorption Efficiency― Physical Review Letters, 2004, 93, 249601; author reply 249602.	7.8	6
472	Ultrafast charge generation in a semiconducting polymer studied withTHzemission spectroscopy. Physical Review B, 2004, 70, .	3.2	36
473	Electron transport inTiO2probed by THz time-domain spectroscopy. Physical Review B, 2004, 69, .	3.2	203
474	Response to "Comment on â€~Coulomb explosion in femtosecond laser ablation of Si(111)'―[Appl. Phys. Lett. 85, 694 (2004)]. Applied Physics Letters, 2004, 85, 696-696.	3.3	7
475	Cascading second-order versus direct third-order nonlinear optical processes in a uniaxial crystal. Optics Communications, 2004, 234, 407-417.	2.1	1
476	Mobility of haloforms on ice surfaces. Chemical Physics Letters, 2004, 385, 244-248.	2.6	20
477	Dephasing of vibrationally excited molecules at surfaces: CO/Ru(001). Chemical Physics Letters, 2004, 388, 269-273.	2.6	15
478	Geometrical vs. statistical models for describing phase transition kinetics in thin films. Physical Chemistry Chemical Physics, 2004, 6, 5516.	2.8	0
479	Broadband Sum Frequency Generation Spectroscopy to Study Surface Reaction Kinetics:Â A Temperature-Programmed Study of CO Oxidation on Pt(111)â€. Journal of Physical Chemistry B, 2004, 108, 14491-14496.	2.6	13
480	Conductivity of solvated electrons in hexane investigated with terahertz time-domain spectroscopy. Journal of Chemical Physics, 2004, 121, 394.	3.0	52
481	Frequency- and time-domain femtosecond vibrational sum frequency generation from CO adsorbed on Pt(111). Journal of Chemical Physics, 2004, 121, 10174-10180.	3.0	30
482	A Molecular View of Cholesterol-Induced Condensation in a Lipid Monolayer. Journal of Physical Chemistry B, 2004, 108, 19083-19085.	2.6	95
483	The Interaction of Water with the Pt(533) Surface. Journal of Physical Chemistry B, 2004, 108, 12575-12582.	2.6	59
484	Theory of bulk, surface and interface phase transition kinetics in thin films. Journal of Chemical Physics, 2004, 121, 1038-1049.	3.0	19
485	Electronic charge transport in sapphire studied by optical-pump/THz-probe spectroscopy. , 2004, , .		9

#	Article	IF	CITATIONS
487	FEMTOSECOND SUM FREQUENCY GENERATION ON MOLECULAR ADSORBATES. , 2004, , .		0
488	Time- vs. frequency-domain femtosecond surface sum frequency generation. Chemical Physics Letters, 2003, 370, 227-232.	2.6	64
489	Coulomb explosion in femtosecond laser ablation of Si(111). Applied Physics Letters, 2003, 82, 4190-4192.	3.3	84
490	Measurement of the Frequency-Dependent Conductivity in Sapphire. Physical Review Letters, 2003, 90, 247401.	7.8	66
491	Vibrational Spectroscopic Investigation of the Phase Diagram of a Biomimetic Lipid Monolayer. Physical Review Letters, 2003, 90, 128101.	7.8	159
492	Vibrational Sum Frequency Scattering from a Submicron Suspension. Physical Review Letters, 2003, 91, 258302.	7.8	135
493	Probing charge carriers in semiconductor quantum dots by terahertz spectroscopy. , 2003, , .		0
494	Phase transitions in a lipid monolayer observed with vibrational sum-frequency generation. , 2003, , .		4
495	Transient Conductivity in Single-Crystal Al2O3 Probed by THz Time-Domain Spectroscopy. Springer Series in Chemical Physics, 2003, , 262-264.	0.2	Ο
496	Lateral interactions between adsorbed molecules: Investigations of CO on Ru(001) using nonlinear surface vibrational spectroscopies. Physical Review B, 2002, 65, .	3.2	35
497	Optimizing Vibrational Population Transfer at Surfaces through Infrared Excitation. Bulletin of the Chemical Society of Japan, 2002, 75, 1005-1010.	3.2	2
498	Real time chemical dynamics at surfaces. Surface Science, 2002, 500, 475-499.	1.9	51
499	Doubly vibrationally resonant spectroscopy of CO on Ru(001). Surface Science, 2002, 502-503, 123-128.	1.9	7
500	Femtosecond time-resolved vibrational SFG spectroscopy of CO/Ru(). Surface Science, 2002, 502-503, 304-312.	1.9	38
501	Electronic charge transport in single-crystal Al2O3: Transient conductivity and its temperature dependence probed by THz time-domain spectroscopy. , 2002, , .		Ο
502	Probing transient conductivity in condensed matter by optical pump/THz time-domain spectroscopy. , 2002, , .		0
503	Ultrafast Surface Dynamics Studied with Femtosecond Sum Frequency Generation. Journal of Physical Chemistry A, 2001, 105, 1683-1686.	2.5	20
504	Charge Transport and Carrier Dynamics in Liquids Probed by THz Time-Domain Spectroscopy. Physical Review Letters, 2001, 86, 340-343.	7.8	88

#	Article	IF	CITATIONS
505	The dynamics of vibrational excitations on surfaces: CO on Ru(001). Journal of Chemical Physics, 2001, 115, 7725-7735.	3.0	55
506	Novel Surface Vibrational Spectroscopy: Infrared-Infrared-Visible Sum-Frequency Generation. Physical Review Letters, 2001, 86, 1566-1569.	7.8	53
507	THz Pump-Probe Measurements of Electrons in Non-Polar Liquids. Springer Series in Chemical Physics, 2001, , 459-463.	0.2	0
508	Hot-band excitation of CO chemisorbed on Ru(001) studied with broadband-IR sum-frequency generation. Chemical Physics Letters, 2000, 325, 139-145.	2.6	47
509	Ultrafast electron dynamics at metal surfaces: Competition between electron-phonon coupling and hot-electron transport. Physical Review B, 2000, 61, 1101-1105.	3.2	187
510	Femtosecond dynamics of chemical reactions at surfaces. Applied Physics A: Materials Science and Processing, 2000, 71, 477-483.	2.3	42
511	Direct Observation of Vibrational Energy Delocalization on Surfaces: CO on Ru(001). Physical Review Letters, 2000, 85, 4341-4344.	7.8	59
512	Femtosecond Surface Vibrational Spectroscopy of CO Adsorbed on Ru(001) during Desorption. Physical Review Letters, 2000, 84, 4653-4656.	7.8	175
513	Desorption of CO from Ru(001) induced by near-infrared femtosecond laser pulses. Journal of Chemical Physics, 2000, 112, 9888-9897.	3.0	102
514	Single-shot measurement of terahertz electromagnetic pulses by use of electro-optic sampling. Optics Letters, 2000, 25, 426.	3.3	163
515	Incoherent Mid-Infrared Photon Echoes With Parametrically Downconverted Light. Laser Chemistry, 1999, 19, 123-126.	0.5	0
516	Phonon- Versus Electron-Mediated Desorption and Oxidation of CO on Ru(0001). Science, 1999, 285, 1042-1045.	12.6	443
517	Coherent picosecond vibron polaritons as probes of vibrational lifetimes. Optics Communications, 1998, 147, 138-142.	2.1	11
518	Dynamical Studies of Zeolitic Protons and Adsorbates by Picosecond Infrared Spectroscopy. Catalysis Reviews - Science and Engineering, 1998, 40, 127-173.	12.9	28
519	Infrared holeburning spectroscopy in acid zeolites. Studies in Surface Science and Catalysis, 1997, 105, 567-574.	1.5	1
520	Dynamical studies of zeolitic protons and interactions with adsorbates by picosecond infrared spectroscopy. Applied Surface Science, 1997, 121-122, 80-88.	6.1	3
521	Picosecond infrared activation of methanol in acid zeolites. Chemical Physics Letters, 1997, 278, 213-219.	2.6	8
522	Dynamics of Infrared Photodissociation of Methanol Clusters in Zeolites and in Solution. The Journal of Physical Chemistry, 1996, 100, 15301-15304.	2.9	22

#	Article	IF	CITATIONS
523	Generation of incoherent mid-infrared photon echoes with parametrically downconverted light. Optics Letters, 1996, 21, 1579.	3.3	1
524	Solvent-dependent vibrational relaxation pathways after successive resonant IR excitation to Ï = 2. Chemical Physics Letters, 1996, 249, 81-86.	2.6	17
525	Vibrational Dephasing Mechanisms in Hydrogen-Bonded Systems. Physical Review Letters, 1996, 76, 2440-2443.	7.8	30
526	Infrared picosecond transient holeâ€burning studies of the effect of hydrogen bonds on the vibrational line shape. Journal of Chemical Physics, 1996, 105, 3431-3442.	3.0	13
527	Enhancement of the vibrational relaxation rate of surface hydroxyls through hydrogen bonds with adsorbates. Chemical Physics Letters, 1995, 233, 309-314.	2.6	31
528	Multiphonon decay of stretch vibrations in zeolites. Chemical Physics, 1995, 201, 215-225.	1.9	9
529	Fast energy delocalization upon vibrational relaxation of a deuterated zeolite surface hydroxyl. Journal of Chemical Physics, 1995, 102, 2181-2186.	3.0	28
530	Time Dependence of Vibrational Relaxation of Deuterated Hydroxyls in Acidic Zeolites Studies in Surface Science and Catalysis, 1994, 84, 493-500.	1.5	9
531	German Commerical Policy Economica, 1935, 2, 353.	1.6	0